Journal of the Serbian Chemical Society
JSCS-info@shd.org.rs • www.shd.org.rs/JSCS

ACCEPTED MANUSCRIPT

This is an early electronic version of an as-received manuscript that has been accepted for publication in the Journal of the Serbian Chemical Society but has not yet been subjected to the editing process and publishing procedure applied by the JSCS Editorial Office.

Please cite this article as T. Kaddour, N. Chaher-Bazizi, S. Zaidi, F. Chebrouk[3], N. Saidene, L. Hanifi, L. Karou, and M. Bachir-Bey, *J. Serb. Chem. Soc.* (2026) https://doi.org/10.2298/JSC260501067K

This "raw" version of the manuscript is being provided to the authors and readers for their technical service. It must be stressed that the manuscript still has to be subjected to copyediting, typesetting, English grammar and syntax corrections, professional editing and authors' review of the galley proof before it is published in its final form. Please note that during these publishing processes, many errors may emerge which could affect the final content of the manuscript and all legal disclaimers applied according to the policies of the Journal.

Journal of the Serbian Chemical Society
JSCS-info@shd.org.rs • www.shd.org.rs/JSCS
J. Serb. Chem. Soc. **00(0)** 1-24 (2026)
JSCS–13940
Original scientific paper
Published DD MM, 2026

Accepted manuscript

Development of a new thin-layer drying model and multicriteria assessment of phytochemical stability and antioxidant activity in olive leaves

TAOUS KADDOUR[1]*, NASSIMA CHAHER-BAZIZI[1], SIDALI ZAIDI[1,2], FARID CHEBROUK[3,4], NAIMA SAIDENE[1], LAMIA HANIFI[1], LYDIA KAROU[1], AND MOSTAPHA BACHIR-BEY[1]

[1]Université de Bejaia, Faculté des Sciences de la Nature et de la Vie, Laboratoire de Biochimie Appliquée, 06000 Bejaia, Algeria, [2]Centre de Recherche en Technologies Agroalimentaires. Route de Targa Ouzemmour, Campus Universitaire, Bejaia, 06000, Algeria, [3]Centre de Recherche Scientifique et Technique en Analyses Physico-Chimiques (CRAPC), BP384, Bou-Ismail, Tipaza 42004, Algeria, and [4]Technical Platform for Physico-chemical Analyzes (PTAPC-Bejaia), Targa Ouzemmour, 06000 Bejaia, Algeria.

(Received 1 May; revised 6 July; accepted 29 October 2026)

Abstract: Olive leaves, a by-product of the olive oil industry, are rich in bioactive compounds whose stability strongly depends on drying conditions. This study models drying kinetics and assesses temperature effects on phytochemical stability and antioxidant activity. Olive leaves were dried using hot air at four temperatures (40, 70, 95, and 120 °C). Drying progress was monitored through continuous mass-loss measurements, and moisture ratios were calculated to characterize drying behavior. These data were fitted to 23 mathematical models, and moisture diffusivity and energy efficiency were determined. Ultrasound-assisted extraction was then performed to evaluate the effect of drying temperature on total phenolics, flavonoids, and antioxidant activity. The proposed kinetic model showed the best agreement with experimental data (R^2= 0.999, $\chi^2 = 1.60 \times 10^{-4}$), demonstrating strong predictive performance. Effective diffusivity increased with temperature, accompanied by a substantial reduction in drying time. Lower temperatures (40 °C) preserved the highest bioactive compound content, while 120 °C markedly accelerated drying (moderate compound loss). Intermediate temperatures (70-95 °C) resulted in the lowest retention due to prolonged thermal exposure.

Keywords: kinetics; mathematical modeling; oven drying; *Olea europaea*; thermal performance.

* Corresponding author. E-mail: taous.kaddour@univ-bejaia.dz
https://doi.org/10.2298/JSC260501067K

INTRODUCTION

Controlling the drying process is essential to preserving the phytochemical contents of medicinal plants. Research on the bioactive compounds of these plants has significantly expanded in recent decades, driven by their therapeutic potential and diverse pharmaceutical applications.[1] *Olea europaea* L., commonly known as the olive tree, has attracted considerable attention due to its recognized medicinal value. Its leaves have been employed in traditional medicine for a wide range of therapeutic uses, particularly in the treatment of ailments such as respiratory disorders and acting as antibacterial agents against certain pathogens. Additionally, olive leaves are recognized for their antidiabetic and hypotensive properties.[2]

The pharmaceutical industry relies heavily on bioactive compounds derived from medicinal plants, including the rich phenolic profile of olive leaves. In the Mediterranean region, olive leaves also represent a valuable resource for the agri-food sector, which plays a pivotal role in cultivating, processing, and valorizing plant-based materials.[3] Consequently, developing effective preservation and processing methods is essential to maintain the stability, functionality, and economic value of these bioactive compounds across various industrial applications, ranging from nutraceuticals to functional foods and natural antioxidants.[2] Therefore, optimizing drying techniques is crucial to preserving their quality and bioactive properties.[4]

Various studies have underscored the importance of optimizing drying parameters for a wide range of agricultural products and medicinal plants, treated by several methods,[5] open-air drying for among other aromatic and medicinal plants,[6,7] as well as microwave drying for various products,[8] such as dehydrated carrot cubes,[9] and potato peels.[10] In the case of olive leaves, several authors have studied optimizing drying conditions, focusing on temperature and drying time to enhance the phytochemical profile.[11] Mathematical modeling of olive leaf drying has been explored using different methods, including solar drying,[12] microwave drying kinetics,[13]and a geothermal dryer.[14]

Although drying plays a crucial role in maintaining the phytochemical and biological characteristics of *Olea europaea* leaves, the impact of combined drying parameters on these qualities is still not fully clarified. This research is structured as follows: (i) investigation of drying kinetics using moisture ratio and drying rate profiles, including the evaluation of drying time and corresponding temperatures, evaluation of 23 standard literature mathematical models alongside a proposed kinetic model to identify the best fit, followed by the determination of activation energy (Ea) and effective moisture diffusivity (D_{eff}); (ii) quan0tification of bioactive compounds, including phenols and flavonoids, along with antioxidant capacity (ABTS, DPPH) after ultrasound-assisted extraction; and (iii) application of Principal Component Analysis (PCA) to explore the relationships between

Accepted manuscript

drying parameters and phytochemical properties. This integrated approach provides a comprehensive multi-criteria assessment of the drying process, balancing efficiency with bioactive compound preservation.

EXPERIMENTAL

Determination of initial moisture content

The initial moisture content (M_0) of *Olea europaea* leaves was determined by oven drying in a ventilated oven. Samples of 15 g were dried at 105 ± 2 °C and weighed at regular intervals until a constant weight was reached. Each measurement was performed in triplicate, and the average weight loss was used to calculate the moisture content on a dry basis (db) according to Equation 1.

$$M_{o.db} = \frac{w_i - w_f}{w_f} \quad (1)$$

Where *Wi* represents the initial weight of the sample (g), and *Wf* denotes the final constant weight after drying (g)

Oven drying procedure

The drying process was carried out in a ventilated oven (Binder® FD53, Germany) at four set temperatures: 40, 70, 95, and 120 °C. The drying duration and temperature were precisely regulated through the oven's digital controls, following established protocols to maintain consistent and uniform drying conditions. At the end of each trial, the final weight of the sample and the equilibrium moisture content of the leaves were determined. Each 15 g sample of olive leaves was spread in a single layer on an aluminum plate and placed in the center of the oven. Moisture loss was measured periodically by weighing the sample at different intervals. Measurements were taken every 30 seconds at 120 °C, every 2 minutes at 95 °C, every 5 minutes at 70 °C, and every 30 minutes at 40 °C. The weighing system used an analytical balance (AS 220.R2, Radwag, Radom, Poland) with a sensitivity of 0.01 g. All experiments were performed in triplicate, with the reported results representing the average values. Drying continued until the sample reached equilibrium moisture content, as indicated by the absence of noticeable changes in weight between successive measurements. After drying, the olive leaves were ground into powder using an electric blender (IKA M20, Staufen, Germany). The resulting powders were stored for further analysis. A schematic overview of the experimental and modeling procedure is presented in Supplementary Figure S1.

Mathematical modeling of drying kinetics

Research on the thin-layer drying of olive leaves, particularly when approached through mathematical modeling, remains insufficiently explored. To expand the range of evaluations and explore additional models, we investigated 23 empirical thin-layer drying models. Experimental drying results for olive leaves under different temperatures were compared with the models in Table I to evaluate their applicability and determine the most accurate fit.

Accepted manuscript

TABLE I. Mathematical models adopted for curve fitting of drying data of olive leaves

N°	Model name	Mathematical equation
1	Aghbashlo *et al.*	$MR = \exp[-k1\ t / (1 + k2\ t)]$
2	Akpinar *et al.*	$MR = a \exp(-k\ t) + (1 - a) \exp(-k\ b\ t)$
3	Chavez-Mendez *et al.*	$MR = [1 - (1 - L2)\ L1\ t]^{(1/(1-L2))}$
4	Fernando and Amarasinghe	$MR = (1 + a\ t + b\ t^2) / (1 + c\ t)$
5	Henderson and Pabis	$MR = a \exp(-k\ t)$
8	Logarithmic	$MR = a \exp(-k\ t) + c$
9	Logistic	$MR = b / [1 + a \exp(k\ t)]$
10	Midilli *et al.*	$MR = a \exp(-k\ t^n) + b\ t$
11	Henderson and Pabis-I	$MR = a \exp(-k\ t) + b\ t$
12	Modified Henderson and Pabis	$MR = a \exp(-k\ t) + b \exp(-k1\ t) + c \exp(-k2\ t)$
13	Page	$MR = \exp(-k\ t^n)$
14	Page-II	$MR = \exp[-(k\ t)^n]$
15	Peleg	$MR = 1 - t / (a + b\ t)$
16	Sledz *et al.*	$MR = b \exp(-k\ t) / [1 + a \exp(k1\ t)]$
17	Modified Midilli *et al.*-I	$MR = a \exp(-k\ t) + b$
18	Two-term exponential	$MR = a \exp(-k0\ t) + (1 - a) \exp(-k1\ a\ t)$
19	Two-term	$MR = a \exp(-k\ t) + b \exp(-k1\ t)$
20	Verma *et al.*	$MR = a \exp(-k\ t) + (1 - a) \exp(-g\ t)$
21	Weibull distribution-I	$MR = a - b \exp[-(k\ t)^n]$
22	Khazaei and Daneshmandi	$MR = a + \exp(-b\ t) - c\ t$
23	Hasibuan and Daud	$MR = 1 - a\ t^n \exp(-k\ t^m)$
	Proposed model (this study)	$MR = [a - b \exp(-k\ t^n)]^{1.5}$

MR – moisture ratio; t – drying time /min; k0, k, k1, k2, g, h – rate constant /min^{-1}; a, b, c, L1, L2 – empirical coefficients; n, m – exponents

Model performance was assessed by fitting them to the experimental curves, which were expressed as moisture ratio (MR) versus time using Equation 2:

$$MR = \frac{M_t - M_e}{M_0 - M_e} \quad (2)$$

Where MR is the moisture ratio; M_t, M_0, and M_e represent the moisture content at any time during drying g H_2O g^{-1} dry matter, the initial moisture content g H_2O g^{-1} DM, and the equilibrium moisture content g H_2O g^{-1} DM, respectively. As the equilibrium moisture content is negligible, it is approximated to zero,[15] allowing the moisture ratio to be simplified as shown in Equation 3.

$$MR = \frac{M_t}{M_0} \quad (3)$$

Drying kinetics rate

Plotting the drying rate (DR) as a function of time provides insight into the characteristic stages of the drying process. The values of DR for olive leaves were calculated by using Equation 4.

$$DR = \frac{M_{t+dt} - M_t}{dt} \quad (4)$$

Accepted manuscript

Where DR is the drying rate / g H_2O g^{-1} DM, M_{t+dt} is the moisture content at time t+dt / g H_2O g^{-1} DM, Mt is the moisture content at time t / H_2O g^{-1} DM, and dt is the time interval / min.

Effective moisture diffusivity

Diffusivity is a key factor in the drying process of olive leaves, determining how moisture moves from the interior of the leaves to the surface for evaporation. It's based on thermodynamic and kinetic principles, particularly Fick's second law for water diffusion, which relates the moisture concentration gradient to the diffusion flux and the effective diffusivity coefficient.

According to Fick's second law for slab-shaped samples, and assuming that the initial moisture is evenly distributed with moisture migration occurring from both sides of the olive leaves, the moisture diffusion process during drying is expressed in Equation 5.[16]

$$\frac{\partial M}{\partial t} = \frac{\partial}{\partial x}\left(D_{eff}\frac{\partial M}{\partial x}\right) \quad (5)$$

The analytical solution, under the assumptions of constant effective diffusivity, negligible shrinkage, and insignificant external resistance to moisture migration, results in a series-form expression for a flat-plate (slab) system, as presented in Equation 6.

$$MR = \frac{8}{\pi^2}\sum_{n=0}^{\infty} -\frac{1}{(2n+1)^2} e^{\left(\frac{(2n+1)^2\pi^2}{4L^2}\right)D_{eff}\times t} \quad (6)$$

For long drying durations, particularly when the MR falls below 0.6, the contribution of higher-order terms in the series solution becomes negligible. Thus, the equation can be accurately approximated by its first term. This simplification is frequently used in studies on the drying behavior of plant materials, particularly during the falling-rate stage, when internal diffusion is the main mechanism of moisture transfer. Under these conditions, the previous expression is reduced to the simplified form presented in Equation 7.

$$MR = \frac{8}{\pi^2} e^{\left(-\frac{\pi^2}{4L^2}D_{eff}\times t\right)} \quad (7)$$

Where MR denotes the dimensionless moisture ratio, 8 represents a positive integer constant in the equation, D_{eff} is the effective moisture diffusivity m^2 s^{-1}, and L is the half-thickness of the olive leaves (L = 0,00022 m).

Applying the natural logarithm to both sides transforms the equation into the linearized form given in Equation 8, which represents a linear relationship between ln(MR) and drying time if D_{eff} remains constant.

$$ln(MR) = ln\frac{8}{\pi^2} - \frac{\pi^2 D_{eff}\times t}{4L^2} \quad (8)$$

However, in this study, the logarithmic plot of MR versus drying time exhibited a nonlinear trend. The effective diffusivity can be obtained by plotting ln(MR) versus drying time t, where the slope of the resulting straight line corresponds to the expression given in Equation 8.

$$Slope = \left(\frac{\pi^2}{4L^2}D_{eff}\right) \quad (9)$$

Using the slope of the graph and the sample thickness, we can deduce the effective diffusion coefficient. The validity of this approach requires that ln (MR) = f (t) be linear. However, in our case, the obtained graphs are not linear, indicating that the diffusivity is not constant and depends on the water content. This is typically observed in biological matrices

Accepted manuscript

with highly porous structures. Consequently, the equation was solved numerically to obtain the Fourier number (F_0), as given in Equation 10.

$$F_0 = -0.101\, ln(MR) - 0.0213 \quad (10)$$

The effective moisture diffusivity was calculated using Equation 11.

$$D_{eff} = \frac{F_0}{\left(\frac{t}{4L^2}\right)} = \frac{-0.101 \times ln(MR) - 0.0213}{\left(\frac{t}{4L^2}\right)} \quad (11)$$

Activation energy

The Arrhenius equation is commonly used to determine the activation energy of moisture diffusion, based on the relationship between temperature and the diffusion coefficient.[17] Accurately measuring the temperature within a ventilated oven drying system can be difficult. The activation energy was calculated using a modified version of the Arrhenius equation, as presented in Equation 12, which can be simplified to Equation 13 for graphical representation.

$$D_{eff} = D_0 e^{\left(\frac{-Ea}{RT}\right)} \quad (12)$$

$$ln\, D_{eff} = ln\, D_0 - \frac{Ea}{RT} \quad (13)$$

Where Ea represents the activation energy / kJ mol^{-1}, D_{eff} is the effective diffusivity / m^2 s^{-1}, D_0 is the pre-exponential factor / m^2 s^{-1}, R is the universal gas constant (8.314 J mol^{-1} K^{-1}), and T is the temperature / K.

Ultrasonic-assisted extraction

The phenolic compounds in the powders obtained from olive leaves dried at the four different temperatures were extracted using an ultrasound bath at 40 kHz (UCI-150, 400 W, R. Espinar SL, Barcelona). The powdered olive leaves were mixed with a 70:30 (v/v) ethanol-water solution at a solid-to-liquid ratio of 1:12.5 g mL^{-1}. Extraction was performed at 45 °C for 10 minutes, followed by centrifugation at 5000 rpm for 10 minutes at 4 °C. The supernatant obtained was carefully removed and saved. The extraction procedure was subsequently repeated twice on the residual plant material. The two ethanolic extracts obtained were combined, and the ethanol was evaporated under reduced pressure using a rotary evaporator. The resulting solution was then lyophilized to produce the dry extract.[18]

Total phenolic and flavonoid contents

The total phenol content (TPC) of the olive leaf extract was quantified using the Folin–Ciocalteu method.[19] Before measurement, extracts were diluted with a 70:30 mixture of ethanol and water (v/v) to achieve appropriate concentrations. Then, 20 µL of the diluted sample was combined with 200 µL of a 10 % Folin–Ciocalteu reagent. After mixing, the mixture was allowed to stand at room temperature for 5 minutes, followed by the addition of 80 µL of 7.5 % sodium carbonate solution. The reaction proceeded for 30 minutes before absorbance was recorded at 760 nm using a microplate reader (Synergy HTX, BioTek, Winooski, VT, USA). The TPC was expressed as mg gallic acid equivalents g^{-1} dry matter (mg GAE g^{-1} DM).

The total flavonoid content (TFC) was measured using a colorimetric assay.[20] A volume of 100 µL of the diluted extract was combined with an equal volume of 2 % aluminum chloride solution. After incubating for 10 minutes, the absorbance of the resulting complex was measured at 430 nm. TFC was expressed as mg rutin equivalents g^{-1} dry matter (mg RE g^{-1} DM). The dosage was performed in both methods using a microplate reader (BioTek Synergy HTX).

Accepted manuscript

Evaluation of antiradical activity

ABTS radical scavenging activity

The ABTS radical solution was prepared according to established protocols by mixing ABTS and potassium persulfate and was allowed to react for 16 hours. Before the assay, the solution was diluted with ethanol to achieve an absorbance of 0.7 ± 0.05 at 734 nm. Then, 20 µL of the extract was mixed with 180 µL of the ABTS solution for the scavenging activity test. The reaction mixture was incubated at 30 °C for 10 minutes to facilitate effective radical scavenging.[21] Following incubation, the absorbance was recorded to determine the radical scavenging activity.

DPPH radical scavenging activity

The antioxidant capacity of the olive leaf extract was evaluated through the DPPH radical scavenging assay. In brief, 20 µL of the extract was mixed with 180 µL of 100 µM DPPH solution. After incubating for 30 minutes, the absorbance was measured at 517 nm. [21]

Antioxidant capacity in the DPPH assay and ABTS assay was expressed as mg gallic acid equivalents g^{-1} dry matter (mg GAE g^{-1} DM).

Statistical analysis

All experiments were conducted in triplicate, and the results are expressed as means ± standard deviations (SD). Descriptive calculations and data processing were performed using Microsoft Excel (Microsoft Office 2019, USA).

Drying kinetics were analyzed by nonlinear regression using STATISTICA software (TIBCO Statistica, version 13.5.0.17, TIBCO Software Inc.) and JMP Pro (version 19, JMP Statistical Discovery LLC). The parameters of the thin-layer drying kinetic models were estimated by non-linear regression using the least squares method via the Levenberg–Marquardt optimization algorithm. To prevent convergence toward local minima and avoid physically unrealistic or erratic parameter values, we specified realistic initial guesses before iteration, based on preliminary estimates derived from the shape of the experimental drying curves. We assessed the goodness of fit of the mathematical models using the coefficient of determination (R^2), reduced chi-square (χ^2), and root mean square error (RMSE), calculated according to Equations 14, 15, and 16, respectively.

$$R^2 = 1 - \frac{\sum_{i=1}^{N}(MR_{exp,i} - MR_{pre,i})^2}{\sum_{i=1}^{N\Sigma}(MR_{exp,i} - \overline{MR}_{exp}()^2)} \quad (14)$$

$$\chi 2 = \sum_{i=1}^{N} \frac{(MR_{pre,i} - MR_{exp,i})^2}{N - Z} \quad (15)$$

$$RMSE = \sqrt{\sum_{i=1}^{N} \frac{(MR_{pre,i} - MR_{exp,i})^2}{N}} \quad (16)$$

Where $MR_{exp,i}$ is the experimental moisture ratio at observation i, $MR_{pre,i}$ is the predicted moisture ratio at this observation, MR_{exp} is the average experimental moisture ratio, and *N* is the number of experimental data points.

Preliminary exploration of the proposed model's fixed exponent (m), including grid-search optimization, multi-start convergence checks, and nested-model comparison (F-test, AIC), figurewas performed in Python (SciPy v1.x, scipy.optimize.curve_fit). Final parameter estimation and statistical validation of the proposed model were then confirmed using JMP Pro 19 (SAS/JMP Statistical Discovery LLC, USA).

Accepted manuscript

For the antioxidant parameters, statistical analyses were performed using one-way analysis of variance (ANOVA), followed by Tukey's HSD test for multiple comparisons, with significance set at $P < 0.05$. Principal component analysis (PCA) was performed using XLSTAT (Microsoft Excel add-in) to explore relationships among the measured variables and identify patterns associated with drying conditions.

RESULTS AND DISCUSSION

Drying kinetics

The drying behavior of olive leaves was first evaluated by monitoring changes in the moisture ratio (MR) as a function of drying time under convective drying conditions. This preliminary assessment provides an overview of the effect of drying temperature on moisture removal and establishes the basis for the subsequent kinetic modeling and estimation of effective moisture diffusivity. The experimental drying curves obtained at 40, 70, 95, and 120 °C are presented in Figure 1.

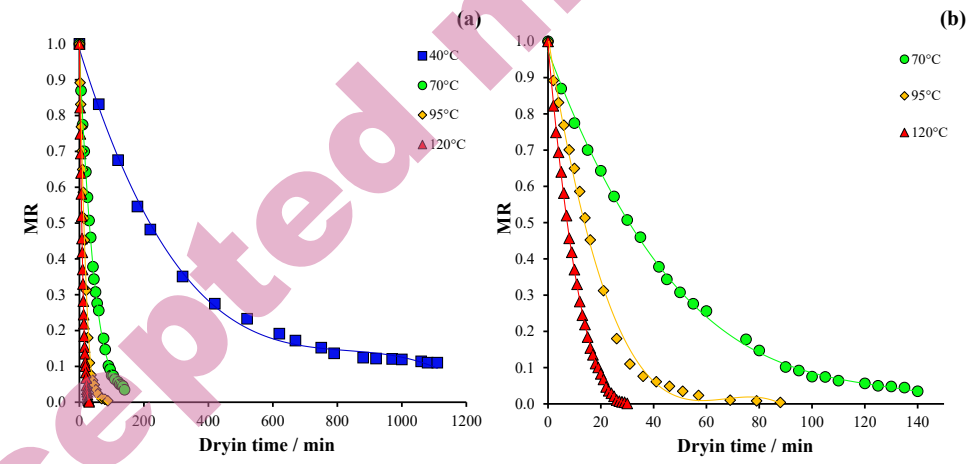

Fig. 1. Experimental drying curves of olive leaves expressed as moisture ratio (MR) as a function of drying time at different drying temperatures (40, 70, 95, and 120 °C).

The initial moisture content of the olive leaves was 0.4713 ± 0.02 g g^{-1} on a Dry Matter (DM). As shown in Figure 1, the moisture ratio decreased progressively with drying time at all temperatures, with a markedly faster decline as the drying temperature increased. The total drying times required to reach the final experimental condition were 1080, 140, 88, and 30 min at 40, 70, 95, and 120 °C, respectively, confirming that increasing the drying temperature substantially accelerated moisture removal.

The temperature-dependent drying behavior indicates that temperature was a major factor controlling the rate of moisture removal from the olive leaves. At higher temperatures, the greater thermal energy supplied to the material enhances

Accepted manuscript

water evaporation and increases the driving force for moisture transfer from the leaf matrix to the surrounding air. Consequently, the drying curves became progressively steeper as the temperature increased from 40 to 120 °C. Similar temperature-dependent increases in drying rate have been reported for plant materials and other plant materials.[22–24]

At 40 °C, moisture removal proceeded considerably more slowly, and the drying process required 1080 min to reach the final experimental condition. The lower drying rate at this temperature can be associated with the lower heat input and reduced vapor-pressure gradient between the product and the surrounding air, which limit water evaporation and subsequent moisture transfer. As drying proceeds, the remaining water becomes increasingly difficult to remove as internal moisture-transfer resistance becomes more significant. The prolonged drying time observed at 40 °C is therefore likely related to the combined effects of a weaker external driving force and increasing internal resistance to moisture migration.[25]

No distinct constant-rate drying period was apparent in the experimental drying curves at any of the temperatures investigated; moisture removal occurred predominantly under falling-rate conditions, with progressively slower moisture removal as drying proceeded. In plant materials, the absence or limited occurrence of a constant-rate period is commonly associated with the rapid removal of readily available surface moisture and the subsequent increasing importance of internal moisture migration.[26,27] Under these conditions, internal moisture transport becomes an important resistance to mass transfer. This falling-rate behavior supports the use of diffusion-based models, including Fick's second law, to estimate the effective moisture diffusivity (D_{eff}) of olive leaves.

Drying rates

To complement the drying-kinetics analysis, the variation in drying rate with moisture content was examined at the four investigated temperatures. The resulting profiles provide additional insight into the changes in moisture-removal rate throughout the drying process and are shown in Figure 2.

Accepted manuscript

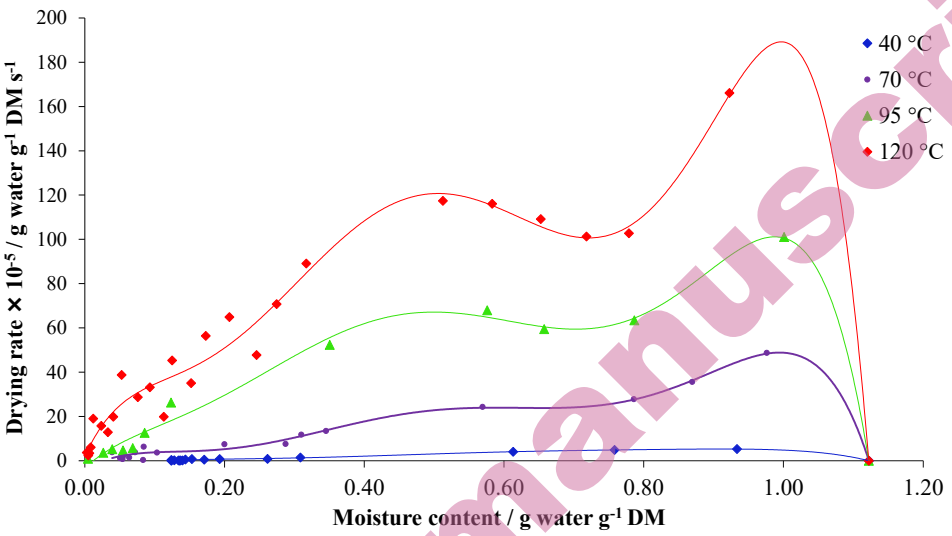

Fig. 2. Variation in drying rate with moisture content of olive leaves during convective drying at 40, 70, 95, and 120 °C.

The drying-rate profiles exhibited a non-linear pattern across the investigated moisture-content range. At all temperatures, the drying rate initially increased, reached a maximum at an intermediate moisture content, and subsequently decreased as the moisture content declined further. However, this decrease was not strictly continuous. At 70, 95, and 120 °C, the overall decline in drying rate was interrupted by several local increases, particularly during the intermediate stages of drying, whereas these fluctuations were considerably less pronounced at 40 °C. This pattern indicates that the rate of moisture removal varied throughout the drying process, with moisture-transfer resistance becoming increasingly important at lower moisture contents. The pronounced decrease in drying rate during the later stages is consistent with the increasing difficulty of removing the remaining moisture from the plant matrix.

A clear temperature-dependent effect was observed in the magnitude of the drying rate. The maximum experimental drying rates increased markedly with increasing temperature, reaching approximately 5.25×10^{-5}, $48.71\ 10^{-5}$, 101.07×10^{-5}, and 166.12×10^{-5} g water g^{-1} DM s^{-1} at 40, 70, 95, and 120 °C, respectively. Thus, the maximum drying rate at 120 °C was approximately 32-fold higher than that at 40 °C. This pronounced increase provides a quantitative indication of the strong temperature dependence of moisture removal under the experimental conditions.

The higher drying rates observed at elevated temperatures can be attributed primarily to enhanced heat transfer and evaporation, together with an increased driving force for moisture transfer between the leaf matrix and the surrounding air. These effects facilitate moisture migration and accelerate overall mass transfer,

Accepted manuscript

thereby reducing the time required to reach the final moisture content, as observed in Figure 1. Similar temperature-dependent drying behavior has been reported for various plant-based and agricultural materials.[26,27] The progressive reduction in drying rate at lower moisture contents also highlights the increasing contribution of internal moisture-transfer resistance during the later stages of drying, which is consistent with the predominantly falling-rate behavior identified from the drying kinetics.

Mathematical modeling of drying kinetics

Drying kinetics modelling provides a means to anticipate the process course and determine its endpoint. Empirical mathematical models, commonly used to describe drying behavior, are widely applied to characterize experimental moisture loss data. In this study, twenty-three drying models were applied to characterize the drying behavior of olive leaves at the four investigated temperatures, and their corresponding parameters are reported in Supplementary Material (Table S1). Based on the fitting performance, the best-performing conventional models were selected according to the highest coefficients of determination (R^2) and the lowest χ^2 and RMSE values.

Among the conventional models, the Hii et al., Midilli et al., Modified Henderson and Pabis, and Weibull models showed particularly good agreement with the experimental drying data. The Hii et al. model provided R^2 values ranging from 0.9988 to 0.9997, with RMSE values of 0.005568–0.016444, while the Midilli et al. model showed similarly high R^2 values (0.9987–0.9996) and RMSE values of 0.007966–0.017595. The Modified Henderson and Pabis and Weibull models also exhibited high coefficients of determination and relatively low error values, confirming their good ability to describe the experimental drying curves. These results indicate that several conventional empirical models can effectively reproduce the non-linear evolution of moisture ratio in olive leaves. However, the relatively close fitting performance of these models suggests that statistical fit alone may not be sufficient to identify a universally superior model. Moreover, empirical models primarily provide mathematical descriptions of the relationship between moisture ratio and drying time, and their parameters do not necessarily have a direct physical interpretation of the underlying moisture-transfer mechanisms.

The good performance of several conventional models across the investigated temperatures also indicates that model suitability may depend on the drying conditions and on the characteristics of the experimental drying curves. Consistent with the findings reported by,[13] the Midilli *et al.* model has been consistently found to be the most suitable for predicting the specific drying kinetics of various agricultural products, including olive leaves.[28] Nevertheless, the present comparison shows that other formulations, particularly the Hii et al. model, can provide similarly strong or even better statistical fits under the conditions

Accepted manuscript

investigated here. Therefore, rather than selecting a conventional model solely on the basis of its statistical performance, the comparison of the 23 models was used as a reference for evaluating the newly proposed drying model.

Validation of the proposed model

The performance of the proposed model was evaluated using the experimental drying data obtained at 40, 70, 95, and 120 °C. Model parameters were estimated by nonlinear regression, and the goodness of fit was assessed using the same statistical criteria employed for the conventional thin-layer drying models, namely the R^2, χ^2, and RMSE. The use of identical evaluation criteria ensured a consistent basis for comparison and enabled the predictive capability of the proposed formulation to be assessed relative to established drying models.

The proposed model is expressed as:

$$MR = [a - b\,exp(-k\,t^n)]^{1.5} \quad (17)$$

The proposed model, derived from the Demir model by introducing a fixed exponent (m = 1.5), was selected based on AIC minimization and validated at all drying temperatures. It consistently outperformed the Newton, Page, Henderson-Pabis, and Logarithmic models, and showed lower AIC values than the standard Demir model (m = 1) without increasing the number of estimated parameters. The model provided an excellent fit to the experimental data, with mean values of R^2=0.999349 ± 0.000421, RMSE = 0.009391 ± 0.004762, and χ^2=0.000160 ± 0.000136. The increase of "k" with temperature agrees with the expected enhancement of moisture transport during convective drying, while variations in n varied with temperature and reached their highest value at 95 °C, indicating a change in the curvature of the drying curves.

The parameters "a" and "b" showed limited dependence on temperature and mainly contributed to improving the flexibility of the model fit. As with many empirical and semi-empirical drying models, these parameters should be interpreted primarily as fitting coefficients rather than directly measurable physical quantities, a behavior also reported for the Logarithmic and Demir models in previous studies. Compared with conventional empirical models, the proposed formulation offers additional flexibility through the exponentiation of the moisture-ratio function, resulting in a more accurate representation of the experimental drying curves. Although the model remains predominantly empirical, its excellent fitting performance and stability across all investigated temperatures support its suitability for describing the drying kinetics of olive leaves. Further validation using other plant materials and drying conditions would be useful to assess its broader applicability.

Effective moisture diffusivity

Diffusivity is a key parameter in the drying process, as it provides an apparent measure of the internal moisture-transfer capacity of the material under the applied

Accepted manuscript

drying conditions. The variation of the effective moisture diffusivity (D_{eff}) with moisture content and drying temperature is presented in Figure 3. The profiles provide additional information on the changes in moisture-transfer behavior observed during the drying process and complement the drying-rate and kinetic analyses presented above.

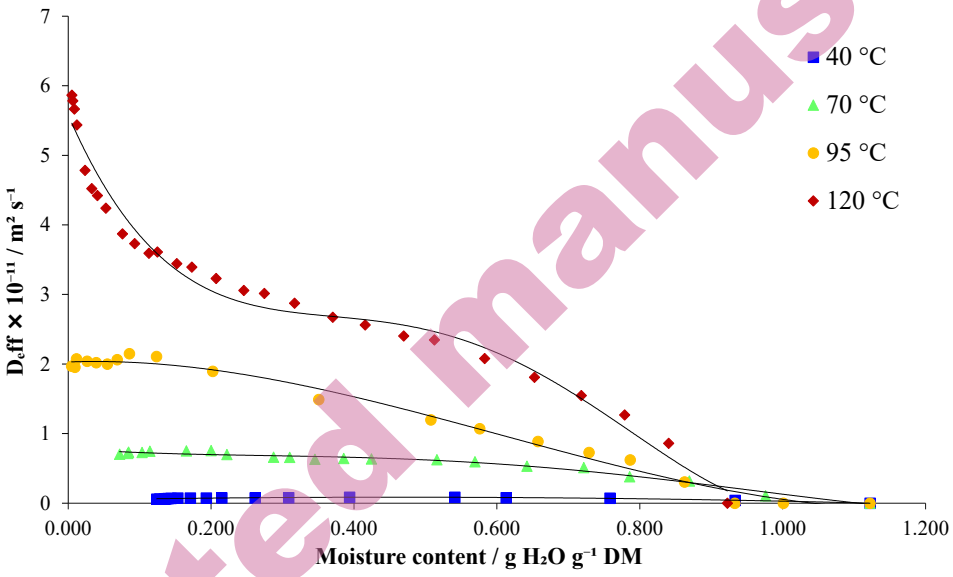

Fig. 3. Variation of effective moisture diffusivity as a function of moisture content during convective drying of olive leaves at 40, 70, 95, and 120 °C.

The D_{eff} exhibited a clear temperature-dependent increase. The average Deff values, calculated over the entire drying process, were 0.070 × 10^{-11} m^2 s^{-1}at 40 °C, 0.557 × 10^{-11} m^2 s^{-1} at 70 °C, 1.255 × 10^{-11} m^2 s^{-1}at 95 °C, and 3.294 × 10^{-11} m^2 s^{-1}at 120 °C, confirming that higher drying temperatures markedly enhanced water molecule mobility within the leaf tissue. To further characterize this behavior, the detailed evolution of D_{eff} as a function of moisture content was examined for each drying temperature. At 40 °C, D_{eff} increased rapidly at the beginning of the drying process, reaching approximately 0.076 × 10^{-11} m^2 s^{-1} at a moisture content of about 0.193 g^{-1} DM, followed by a gradual decrease toward lower moisture contents. At 70 °C, D_{eff} increased progressively from approximately 0.756× 10^{-11} at 0.114 g g^{-1} DM of moisture content, although moderate fluctuations were observed at the lowest moisture contents. At 95 °C, the increase was more pronounced, with D_{eff} reaching approximately 2.14 × 10^{-11} m^2 s^{-1}at a moisture content of about 0.085 g g^{-1} DM, followed by a slight decrease and subsequent stabilization. The strongest increase was observed at 120 °C, where D_{eff} rose progressively to approximately 5.86 × 10^{-11} m^2 s^{-1} at low moisture

Accepted manuscript

content. These profiles indicate that the magnitude and evolution of D_{eff} depend strongly on both temperature and the moisture state of the leaves.

The increase in D_{eff} with increasing temperature is consistent with the higher drying rates observed in Figure 2 and the shorter drying times reported in Figure 1. Higher temperatures increase the energy available for moisture removal and enhance the driving force for internal moisture migration. In addition, temperature-dependent changes in water viscosity and molecular mobility may facilitate moisture movement through the leaf matrix. The particularly pronounced increase in D_{eff} at 95 and 120 °C suggests that thermal conditions strongly affect the apparent internal mass-transfer properties of the leaves. The porous and heterogeneous structure of plant tissues may further contribute to this behavior by providing interconnected pathways for moisture transport.[29] Moreover, elevated drying temperatures accelerate water evaporation and can modify the moisture-transfer resistance within the material, thereby increasing the apparent effective diffusivity.[30]

The D_{eff} values obtained in the present study are consistent with the general range reported for food and agricultural materials (10^{-12} to 10^{-9} m^2 s^{-1}), particularly at the lower end typical of leafy materials dried under moderate temperatures.[31] The values obtained for olive leaves are therefore within a physically plausible range and are comparable to those reported for similar materials. Ben Haj Said et al. reported D_{eff} values ranging from $2{,}55 \times 10^{-12}$ to $8{,}83 \times 10^{-12}$ m^2 s^{-1} in *Allium roseum*, [32] which are of the same order of magnitude as the values obtained in the present study.

An important feature of Figure 3 is that D_{eff} did not remain constant throughout drying. At several temperatures, particularly 40 and 95 °C, the diffusivity changed as the moisture content decreased rather than following a simple monotonic trend. This behavior indicates that the apparent resistance to moisture transfer evolves during drying and that a constant-D_{eff} assumption may not adequately represent the entire drying process. Such behavior can be associated with changes in moisture binding, tissue structure, porosity, and the relative contribution of different moisture-transport mechanisms as drying progresses.[33] At higher temperatures, the marked increase in D_{eff} toward lower moisture contents may also reflect the combined effects of enhanced thermal energy and changes in the internal structure of the leaves during drying.

The observed dependence of D_{eff} on moisture content has an important implication for the mathematical description of olive-leaf drying. Rather than treating diffusivity as a single constant characteristic of a given temperature, considering D_{eff} as a variable parameter provides a more realistic representation of the changing internal moisture-transfer conditions. This observation is also consistent with the non-linear behavior of the ln(MR)-versus-time relationship observed in the present study. Accordingly, the moisture-dependent diffusivity

Accepted manuscript

profiles provide additional support for the development and application of a drying model capable of describing the changing kinetics of olive leaves over the entire moisture range.

Activation energy

The activation energy (E_a) was determined using Eq. (9) and estimated by a graphical method based on the relationship between ln(D_{eff}) and the reciprocal of absolute temperature (T^{-1}), where T is expressed in Kelvin, as illustrated in Figure 4. The activation energy provides an indication of the temperature sensitivity of moisture diffusion during the drying process and is commonly estimated from the slope of the Arrhenius relationship.

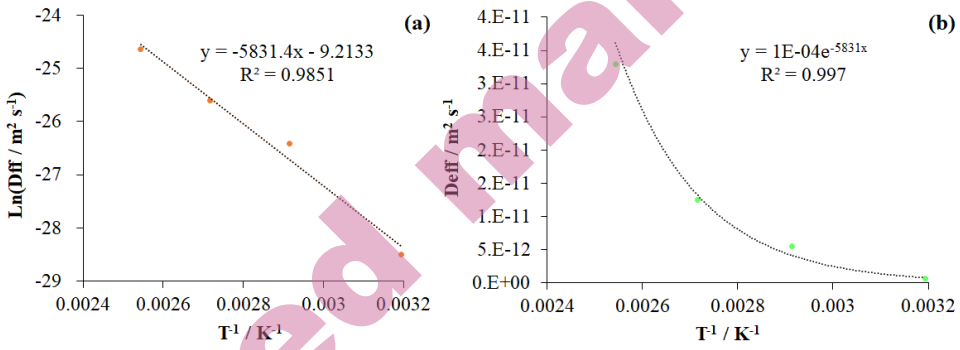

Fig. 4. Arrhenius relationships describing the temperature dependence of effective moisture diffusivity during convective drying of olive leaves: (a) linearized plot of ln(D_{eff}) versus (T^{-1}) and (b) exponential relationship between D_{eff} and T^{-1}.

The calculated E_a values were 44.50 kJ mol^{-1} using the equation-based method and 48.48 kJ mol^{-1} using the graphical method, giving a mean value of 46.49 ± 1.99 kJ mol^{-1}. The relatively close values obtained by the two approaches indicate good consistency between the calculation methods. The magnitude of E_a obtained in the present study is within the range reported for the drying of plant-based materials and is comparable with values previously reported for olive leaves.[34,35] Bennaceur *et al.* reported activation energies of 62.23 ± 1.78 kJ mol^{-1} without ultrasound and 43.83 ± 1.42 kJ mol^{-1} with ultrasound during olive-leaf drying.[17] The drying process aligns with the typical energy requirements for moisture evaporation during drying. Various factors influence

The obtained E_a value indicates that the effective moisture diffusivity of olive leaves is sensitive to temperature, consistent with the pronounced increase in D_{eff} observed as the drying temperature increased from 40 to 120 °C. The temperature dependence of moisture transport reflects the combined effects of increased molecular mobility, enhanced evaporation, and changes in the internal moisture-transfer resistance of the leaf matrix. Environmental and process conditions,

Accepted manuscript

including temperature and relative humidity, can also influence moisture-transfer behavior and consequently affect the estimated activation energy.[30]

The close agreement between the two approaches used to estimate E_a, together with its consistency with previously reported values, supports the reliability of the estimated temperature dependence of D_{eff} for the olive-leaf drying process.

Total phenol content and total flavonoid content

The total phenolic content of olive leaves dried at different convective drying temperatures is presented in Figure 5a. Drying temperature significantly affected the phenolic content of the samples ($p < 0.05$). The highest TPC was recorded at 40 °C (85.00 ± 4.91 mg GAE g^{-1} DM). Increasing the drying temperature to 70 °C resulted in a pronounced decrease in TPC, which reached its lowest value of 52.34 ± 3.34 mg GAE g^{-1} DM. At higher temperatures, TPC increased again to 60.37 ± 0.51 and 67.20 ± 2.03 mg GAE g^{-1} DM at 95 and 120 °C, respectively. Thus, TPC exhibited a non-linear response to drying temperature, following the order 40 > 120 > 95 > 70 °C.

This pattern suggests that drying temperature influences the balance between thermal degradation and the release or extractability of phenolic compounds from the plant matrix. The lower TPC observed at 70 and 95 may be related to partial thermal degradation of heat-sensitive compounds before sufficient structural disruption occurs to enhance their release.[36] Indeed, drying time, temperature, and the structural integrity of the plant matrix can influence the retention of phenolic compounds. Short drying times at high temperatures or prolonged drying at mild temperatures may favor their preservation, whereas extended exposure at intermediate temperatures may promote degradation. At elevated temperatures, rapid cellular breakdown can enhance the release of bound phenolics, while lower temperatures favor the preservation of thermolabile compounds.[37] The observed pattern may therefore result from the combined effects of temperature, drying duration, structural changes in the plant matrix, and compound extractability. Consistent with the TPC behavior observed in the present study on olive leaves, [38] also found that intermediate oven-drying temperatures reduced the phenolic content of *Laurus nobilis* leaves, with the best results obtained at open-air drying and 120 °C.

Flavonoids, an important subclass of phenolic compounds with recognized antioxidant properties, showed a temperature-dependent pattern consistent with that observed for TPC (Figure 5b). The highest total flavonoid content was measured in leaves dried at 40 °C (7.71 ± 0.20 mg RE g^{-1} DM), followed by 120 and 95, while the lowest value was observed at 70, resulting in the same order of 40 > 120 > 95 > 70 °C. The similar trends observed for TPC and TFC support the role of drying temperature and duration in determining the balance between compound preservation, degradation, and extractability.

Accepted manuscript

Determination of total antioxidant capacity

The antioxidant activity of olive leaves dried at different temperatures was assessed using the ABTS and DPPH assays (Fig. 5c, d). Both assays showed a similar temperature-dependent pattern, with the highest activity at 40 °C, followed by a marked decrease at 70 and 95 °C, which showed similar values, and a subsequent increase at 120 °C. For ABTS, the activity decreased from 24.04 ± 0.81 mg GAE g^{-1} DM at 40 °C to 16.64 ± 0.75 mg GAE g^{-1} DM at 70 °C, before increasing to 20.70 ± 0.40 mg GAE g^{-1} DM at 120 °C. DPPH showed the same pattern, decreasing from 23.49 ± 0.87 mg GAE g^{-1} DM at 40 °C to 15.11 ± 1.37 mg GAE g^{-1} DM at 70 °C and subsequently increasing to 20.73 ± 0.20 mg GAE g^{-1} DM at 120 °C.

The trends observed for ABTS and DPPH closely followed those observed for TPC and TFC, with the highest values at 40 °C, a marked decrease at 70 and 95 °C, and a subsequent increase at 120 °C. The lower antioxidant activity at intermediate temperatures may therefore be related to the reduction in phenolic and flavonoid contents, particularly the loss or reduced extractability of heat-sensitive compounds. In contrast, the recovery observed at 120 °C may be partly associated with the shorter drying time, which limits thermal exposure, together with greater disruption of the plant matrix and enhanced release of antioxidant compounds. [39, 40] These observations are consistent with the influence of drying conditions on antioxidant activity reported by Stępień et al.[41] and Razola-Díaz et al.[35].

Multivariate statistical analysis

Principal component analysis was performed using the Pearson correlation matrix to explore the relationships among drying characteristics, phenolic compounds, and antioxidant responses, and to discriminate the olive leaf samples according to drying temperature (Figure 6). The first two principal components (PC1 and PC2) accounted for 63.62% and 33.17% of the total variance, respectively, explaining 96.79% of the overall variability. Thus, the first two components provided a comprehensive representation of the multivariate structure of the dataset.

PC1 was mainly characterized by positive associations with drying time, TPC, ABTS, DPPH, and TFC, whereas mass loss was negatively associated with this component. Drying time showed the strongest correlation with PC1 (r = 0.968), followed by TPC (r = 0.948), ABTS (r = 0.930), DPPH (r = 0.878), and TFC (r = 0.784). These variables therefore defined a common positive dimension associated with drying duration and the preservation of phenolic and antioxidant characteristics. PC2 provided a complementary drying-related dimension, being strongly and positively associated with D_{eff} (r = 0.853) and mass loss (r = 0.690), while DR showed a strong negative association (r = −0.774). TFC also contributed positively to PC2 (r = 0.606).

Accepted manuscript

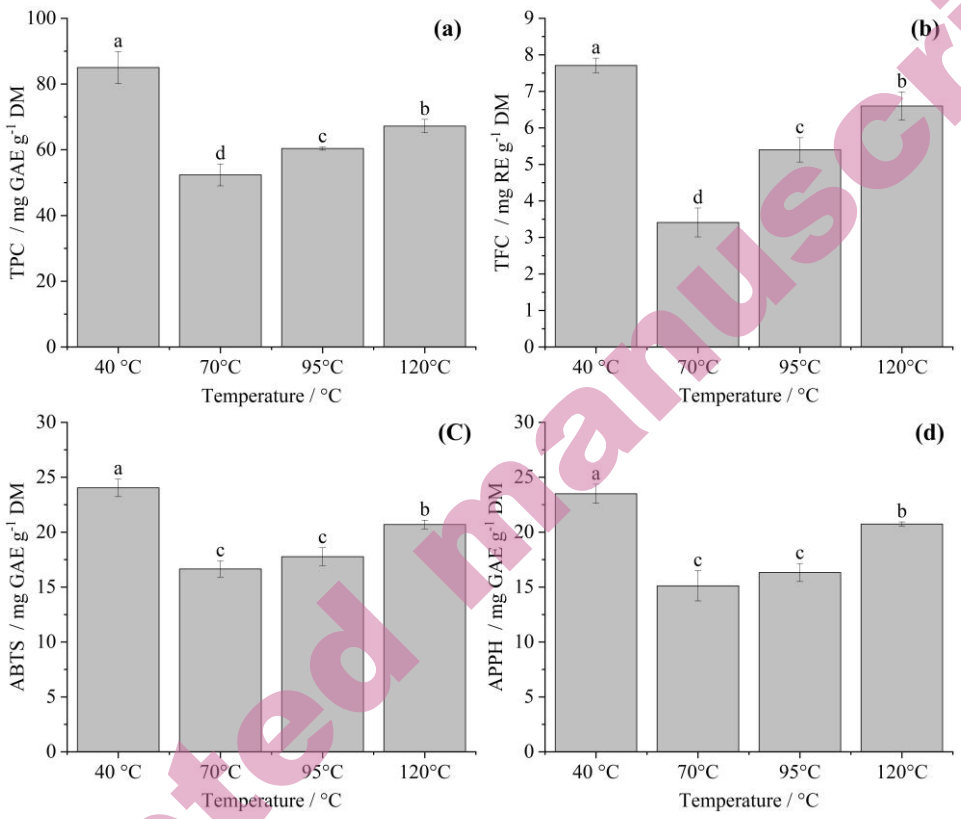

Fig. 5. Effect of drying temperature on the biological responses of olive leaves: (a) total phenolic content (TPC), (b) total flavonoid content (TFC), (c) ABTS radical scavenging activity (ABTS), and (d) DPPH radical scavenging activity (DPPH). For each parameter, values with different letters are significantly different (one-way ANOVA followed by Tukey's HSD test, $P < 0.05$).

The orientation of the variables in the biplot revealed a close grouping of TPC, TFC, ABTS, and DPPH, indicating strong positive associations among these responses. This pattern was supported by the Pearson correlation matrix, which showed strong correlations between TPC and ABTS ($r = 0.986$), TPC and DPPH ($r = 0.959$), TPC and TFC ($r = 0.940$), as well as between ABTS and DPPH ($r = 0.991$). The drying-related variables also showed marked relationships, particularly the strong negative correlation between mass loss and DR ($r = -0.992$), while mass loss was positively correlated with D_{eff} ($r = 0.799$). These relationships indicate that the multivariate variation in the dataset was determined by two closely related dimensions involving, respectively, biological responses and drying characteristics.

Accepted manuscript

The distribution of the drying treatments within the PCA space further highlighted their distinct multivariate profiles. The 40 °C treatment was clearly separated from the other treatments along PC1, with a score of 3.329, and was closely associated with the group of phenolic and antioxidant variables as well as with drying time. This position is consistent with the favorable biological response observed at this temperature. In contrast, the 70 °C treatment was located in the lower-left quadrant, with negative scores on both PC1 and PC2, reflecting its comparatively lower phenolic and antioxidant responses. The 95 °C treatment was positioned close to the origin, indicating a more intermediate profile across the variables represented by the first two components.

The 120 °C treatment was located in the upper-left quadrant and showed a strong positive association with PC2 (score = 2.001), reflecting a drying profile characterized particularly by the positive contributions of D_{eff} and mass loss. At the same time, its position remained relatively close to the phenolic and antioxidant variables in the biplot, consistent with its comparatively high biological responses. Thus, the 120 °C treatment represents a distinct combination of enhanced drying-related characteristics and relatively well-preserved phenolic and antioxidant responses, rather than a simple contrast between drying efficiency and biological quality.

The PCA provides a clear basis for differentiating the drying temperatures according to the balance between drying efficiency and preservation of functional characteristics. Drying at 40 °C was the most favorable condition for preserving phenolic and flavonoid compounds and maintaining antioxidant activity, although this benefit was associated with a substantially longer drying time. In contrast, 120 °C markedly reduced the drying time while still maintaining relatively high phenolic and antioxidant responses, making this condition a promising alternative when processing efficiency is prioritized. Drying at 95 °C provided an intermediate option, with a considerably shorter drying time than at 40 °C but only moderate preservation of the bioactive characteristics. The 70 °C treatment appeared the least advantageous overall, as it required a longer drying time than the higher-temperature treatments while being associated with the lowest retention of phenolic and flavonoid compounds and the lowest antioxidant activity. Taken together, these results suggest that the selection of the drying temperature should consider the intended balance between product quality and processing efficiency: 40 °C is preferable when maximum preservation of functional compounds is the primary objective, whereas 120 °C offers a more favorable compromise between rapid drying and retention of bioactive properties.

Accepted manuscript

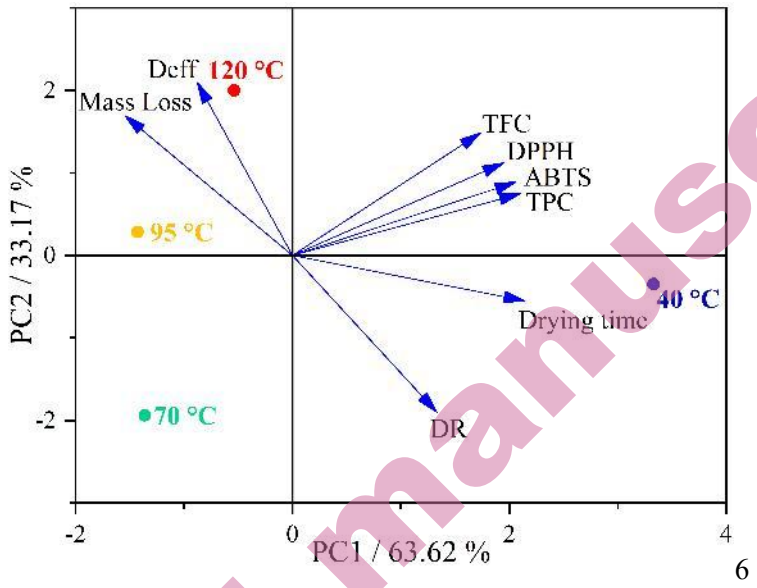

Fig. 6. Principal component analysis biplot of olive leaves subjected to convective drying at 40, 70, 95, and 120 °C. TPC, total phenolic content; TFC, total flavonoid content; DR, drying rate; D_{eff}, effective moisture diffusivity; ABTS, ABTS radical scavenging activity; DPPH, DPPH, radical scavenging activity.

CONCLUSION

This study presents an integrated approach to optimizing the drying process of *Olea europaea* L. leaves by integrating biological properties with advanced mathematical modeling. A multimodal and multi-criteria approach revealed strong interrelations between drying parameters, bioactive compound retention, and drying efficiency. These findings suggest that lower drying temperatures (40 °C) are most effective for preserving phenolic compounds, flavonoids, and antioxidant activities (DPPH, ABTS), making this condition suitable for laboratory-scale applications or quality-driven uses, such as functional foods and nutraceuticals, where processing time is not a constraint. At 120 °C, the very short exposure time (flash-drying) limited the duration available for thermal degradation despite the high temperature, resulting in only a moderate reduction in bioactive compound content while substantially accelerating moisture removal, drying rate, and effective diffusivity. This condition is therefore optimal at industrial scale, where process speed and energy efficiency are decisive. By contrast, the intermediate temperatures (70 and 95 °C) combined a thermal level high enough to trigger degradation with prolonged exposure times (88–140 min), leading to the lowest bioactive compound retention among the four conditions tested. This highlights that bioactive degradation is governed not by temperature alone, but by the cumulative time–temperature exposure during drying.

Accepted manuscript

Among all drying models tested, a proposed model provided the best fit to the experimental moisture ratio data, yielding an excellent. The activation energy (Ea = 46.49 ± 1.99 kJ mol^{-1}) falls within the typical range reported for plant leaf materials, indicating a moderate energy barrier for moisture diffusion during drying. From a kinetic standpoint, DR and D_{eff} increased markedly with temperature, while drying time and mass loss varied accordingly, confirming the strong influence of temperature on drying kinetics.

These results highlight the importance of balancing biological, technical, and environmental parameters to tailor sustainable drying systems to the intended application, supporting the valorization of *Olea europaea* L. within a circular bioeconomy, both in traditional Mediterranean and emerging olive-growing regions. Future research should incorporate metabolomic profiling to validate these findings at the molecular level, and conduct large-scale, thin-layer drying trials under industrial conditions to confirm their applicability and further improve bioactive compound stability.

NOMENCLATURE

a, b, c, d, k, n, m	Constants
ABTS	2,2′-azino-bis(3-ethylbenzothiazoline-6-sulfonic acid) radical scavenging assay / mg GAE g^{-1} DM
D_{eff}	Effective diffusivity / m^2 s^{-1}
DPPH	2,2-diphenyl-1-picrylhydrazyl radical scavenging activity / mg GAE g^{-1} DM
DR	Drying rate / g H_2O g^{-1} DM
Ea	Activation energy / kJ mol^{-1}
ER	Evaporation rate / g min^{-1}
L	Half thickness of the layer / m
M	Moisture loss of the sample / kg
MC	Moisture content / g H_2O g^{-1} DM
MR	Moisture ratio (dimensionless)
MR exp	Experimental moisture ratio
MR pre	Predicted moisture ratio
mt	Mass of the sample at time t / g
mt+dt	Mass of the sample at time t + dt / g
mw	Mass of evaporated water / kg
n	Constant, positive integer
R^2	Coefficient of determination
RMSE	Root mean square error
T	Temperature / °C
t	Time / s
TFC	Total flavonoid content / mg RE g^{-1} DM
TPC	Total phenolic content / mg GAE g^{-1} DM
Wi	Initial weight of the sample / g
Wf	Final constant weight of the dried sample / g
Z	Number of constants and coefficients
χ^2	Reduced chi-square

Accepted manuscript

SUPPLEMENTARY MATERIAL

Additional data are available electronically at the pages of journal website: https://www.shd-pub.org.rs/index.php/JSCS/article/view/13940, or from the corresponding author on request.

Acknowledgment: The authors gratefully acknowledge the support of the Ministry of Higher Education and Scientific Research (DGRSDT) and the Laboratory of Applied Biochemistry.

И З В О Д

РАЗВОЈ НОВОГ МОДЕЛА СУШЕЊА У ТАНКОМ СЛОЈУ И ВИШЕКРИТЕРИЈУМСКА ПРОЦЕНА СТАБИЛНОСТИ ФИТОХЕМИЈСКИХ ЈЕДИЊЕЊА И АНТИОКСИДАТИВНЕ АКТИВНОСТИ У ЛИСТОВИМА МАСЛИНЕ

TAOUS KADDOUR[1], NASSIMA CHAHER-BAZIZI[1], SIDALI ZAIDI[1,2], FARID CHEBROUK[3,4], NAIMA SAIDENE[1], LAMIA HANIFI[1], LYDIA KAROU[1], и MOSTAPHA BACHIR-BEY[1]

[1]Université de Bejaia, Faculté des Sciences de la Nature et de la Vie, Laboratoire de Biochimie Appliquée, 06000 Bejaia, Algeria, [2]Centre de Recherche en Technologies Agroalimentaires. Route de Targa Ouzemmour, Campus Universitaire, Bejaia, 06000, Algeria, [3]Centre de Recherche Scientifique et Technique en Analyses Physico-Chimiques (CRAPC), BP384, Bou-Ismail, Tipaza 42004, Algeria, and [4]Technical Platform for Physico-chemical Analyzes (PTAPC-Bejaia), Targa Ouzemmour, 06000 Bejaia, Algeria.

Листови маслине, споредни производ индустрије за производњу маслиновог уља, богати су биоактивним једињењима чија стабилност у великој мери зависи од услова сушења. У овом истраживању моделована је кинетика сушења и процењен је утицај температуре на стабилност фитохемијских једињења и њихову антиоксидативну активност. Листови маслине сушени су загрејаним ваздухом на четири температуре (40, 70, 95 и 120 °C). Напредовање процеса сушења праћено је континуираним мерењем губитка масе, а израчунати су односи садржаја влаге ради карактеризације понашања материјала током сушења. Добијени подаци апроксимирани су помоћу 23 математичка модела, а одређени су и ефективна дифузивност влаге и енергетска ефикасност. Након тога, спроведена је екстракција потпомогнута ултразвуком како би се проценио утицај температуре сушења на укупан садржај фенолних једињења, флавоноида и антиоксидативну активност. Предложени кинетички модел показао је најбоље слагање са експерименталним подацима ($R^2 = 0{,}999$, $\chi^2 = 1{,}60 \times 10^{-4}$), што указује на високу предиктивну способност модела. Ефективна дифузивност влаге повећавала се са порастом температуре, уз значајно скраћење времена сушења. Највећи садржај биоактивних једињења очуван је при нижој температури (40 °C), док је сушење на 120 °C значајно убрзало процес, уз умерен губитак једињења. При средњим температурама (70–95 °C) забележено је најмање задржавање биоактивних једињења услед продуженог излагања топлоти.

(Примљено 1. маја; ревидирано 6. јула; прихваћено 29. октобра 2026.)

Accepted manuscript

REFERENCES

1. K. Mazur, B. Kusznierewicz, D. Martysiak-Żurowska, I. Drążkowska, E. Malinowska-Pańczyk, *Nutrients* **16** (2024) 1–16 (https://doi.org/10.3390/nu16101455)
2. M. M. Özcan, B. Matthäus, *Eur. Food Res. Technol.* **243** (2017) 89–99 (https://doi.org/10.1007/s00217-016-2726-9)
3. J. M. Silvan, E. Guerrero-Hurtado, A. Gutierrez-Docio, M. Prodanov, A. J. Martinez-Rodriguez, *Antibiotics* **12** (2023) 26 (https://doi.org/10.3390/antibiotics12010026)
4. Z. Qamar, A. Munir, T. Langrish, A. Ghafoor, M. Tahir, *Agricuture* **13** (2023) 387 (https://doi.org/10.3390/agriculture13020387)
5. V. Patel, K. B. Judal, H. Panchal, B. Singh, A. Jomde, A. Kumar, A. Patel, R. Jain, K. K. Sadasivuni, *Environ. Chall.* **13** (2023) 100778 (https://doi.org/10.1016/j.envc.2023.100778)
6. A. Madan, A. Pare, N. Gowd, *Res. Rev. J. Bot.* **3** (2014) 1–9 (https://sciencejournals.stmjournals.in/index.php/RRJoB/article/view/963)
7. S. Marcelino, S. Hamdane, P. D. Gaspar, A. Paço, *Sustainability* **15** (2023) 14095 (https://doi.org/10.3390/su151914095)
8. C. Kumar, M. A. Karim, *Crit. Rev. Food Sci. Nutr.* **59** (2019) 379–394 (https://doi.org/10.1080/10408398.2017.1373269)
9. J. Huang, M. Zhang, B. Adhikari, Z. Yang, *Food Eng.* **172** (2016) 188–198 (https://doi.org/10.1016/j.jfoodeng.2015.12.023)
10. F. Brahmi, I. Mateos-Aparicio, K. Mouhoubi, S. Guemouni, T. Sahki, F. Dahmoune, F. Belmehdi, C. Bessai, K. Madani, L. Boulekbache-Makhlouf, *Antioxidants* **12** (2023) 638 (https://doi.org/10.3390/antiox12030638)
11. F. S. Markhali, *Processes* **9** (2021) 1662 (https://doi.org/10.3390/pr9091662)
12. B. Nourhène, K. Mohammed, K. Nabil, *Food Bioprod. Process.* **86** (2008) 176–184 (https://doi.org/10.1016/j.fbp.2007.10.001)
13. R. Lemus-Mondaca, L. Zura-Bravo, K. Ah-Hen, K. Di Scala, *J. Sci. Food Agric.* **101** (2021) 6484–6495 (https://doi.org/10.1002/jsfa.11320)
14. H. U. Helvaci, A. Menon, L. Y. Aydemir, F. Korel, G. G. Akkurt, *Energy Procedia* **161** (2019) 108–114 (https://doi.org/10.1016/j.egypro.2019.02.065)
15. A. Özkan-Karabacak, B. Acoğlu-Çelik, T. Özdal, P. Yolci-Ömeroğlu, Ö. U. Çopur, A. Baştuğ-Koç, R. Pandiselvam, *J. Food Biochem.* **2023** (2023) 6531838 (https://doi.org/10.1155/2023/6531838)
16. J. Crank, *The Mathematics of Diffusion (2nd Edition)*, Oxford University Press (1975)
17. S. Bennaceur, A. Berreghioua, L. Bennamoun, A. Mulet, B. Draoui, M. Abid, J. A. Carcel, *Energies* **14** (2021) 1329 (https://doi.org/10.3390/en14051329)
18. C. Zhang, J. Zhang, X. Xin, S. Zhu, E. Niu, Q. Wu, T. Li, D. Liu, *Front. Nutr.* **9** (2022) (https://doi.org/10.3389/fnut.2022.854680)
19. S. Zaidi, N. Chaher-Bazizi, T. Kaddour, Z. Medjahed, N. Benaida-Debbache, *Sustain. Chem. Pharm.* **41** (2024) 101678 (https://doi.org/10.1016/j.scp.2024.101678)
20. L. Hanifi, N. Chaher-Bazizi, Y. Bellik, L. Karou, T. Kaddour, N. Saidene, D. Kilani-Atmani, D. Atmani, M. Bachir-bey, *J. Food Sci.* **90** (2025) e70300 (https://doi.org/10.1111/1750-3841.70300)

Accepted manuscript

21. N. Saidene, N. Chaher-Bazizi, R. Kadi, D. Atmani-Kilani, D. Atmani, S. Zaidi, T. Kaddour, M. Rahmani-Berboucha, N. Debbache-Benaida, S. Bouadam, B. Farhi-Bouadam, M. Bachir-bey, *Chem. Pap.* **78** (2024) 9325 (https://doi.org/10.1007/s11696-024-03745-3)
22. A. Cagliari, T. R. Martiny, R. Nascimento, M. M. Morais, G. Silveira, *Braz. J. Food Technol.* **25** (2022) 1–16. (https://doi.org/10.1590/1981-6723.1472)
23. J. da S. Moura, R. P. e. Sousa, L. H. da S. Martins, C. E. F. da Costa, R. C. Chisté, A. S. Lopes, *Foods* **12** (2023) 1–14 (https://doi.org/10.3390/foods12071452)
24. R. P. F. Chaves, A. L. de Araújo, A. S. Lopes, R. da S. Pena, *Plants* **12** (2023) 127 (https://doi.org/10.3390/plants12010127)
25. R. Battino, D. A. Dolson, M. R. Hall, T. M. Letcher, *J. Chem. Educ.* **84** (2007) 822–825 (https://doi.org/10.1021/ed084p822)
26. A. Motevali, S. Minaei, A. Banakar, B. Ghobadian, H. Darvishi, *J. Saudi Soc. Agric. Sci.* **15** (2016) 179–187 (https://doi.org/10.1016/j.jssas.2014.11.003)
27. E. A. A. Elhussein, S. Şahin, *Heat Mass Transf.* **54** (2018) 1901–1911 (https://doi.org/10.1007/s00231-018-2278-6)
28. K. Altay, A. A. Hayaloglu, S. N. Dirim, *Heat Mass Transf.* **55** (2019) 2173–2184 (https://doi.org/10.1007/s00231-019-02570-9)
29. M. I. H. Khan, C. P. Batuwatta-Gamage, M. A. Karim, Y. T. Gu, *Energies* **15** (2022) 9347 (https://doi.org/10.3390/en15249347)
30. A. Boukhiar, S. Benamara, Y. Bouchal, K. Touderte, S. Messouidi, *Period. Polytech. Chem. Eng.* **66** (2022) 660–674 (https://doi.org/10.3311/PPch.20264)
31. A. M. Abi-Khattar, H. N. Rajha, R. M. Abdel-Massih, R. Habchi, R. G. Maroun, E. Debs, N. Louka, *Food Chem.* **342** (2021) 128236 (https://doi.org/10.1016/j.foodchem.2020.128236)
32. H. Darvishi, J. Khodaei, M. Azadbakht, *Philipp. Agric. Sci.* **98** (2015) 60–72
33. M. Fikry, S. Benjakul, S. Al-Ghamdi, M. Tagrida, T. Prodpran, *Foods* **12** (2023) 3024 (https://doi.org/10.3390/foods12163024)
34. M. del C. Razola-Díaz, V. Verardo, A. M. Gómez-Caravaca, B. García-Villanova, E. J. Guerra-Hernández, *Foods* **12** (2023) 500 (https://doi.org/10.3390/foods12030500)
35. Z. Gharaie, M. H. Azizi, M. Barzegar, H. Ahmadi Gavlighi, *LWT* **105** (2019) 265–271 (https://doi.org/10.1016/j.lwt.2019.02.025)
36. K. Mouhoubi, L. Boulekbache-Makhlouf, W. Mehaba, H. Himed-Idir, K. Madani, *J. Food Process Eng.* **45** (2022). (https://doi.org/10.1111/jfpe.13932)
37. C. He, H. Wang, Y. Yang, Y. Huang, X. Zhang, M. Arowo, J. Ye, N. Zhang, M. Xiao, *Pharmaceutics* **13** (2021) 335 (https://doi.org/10.3390/pharmaceutics13030335)
38. A. E. Stępień, J. Gorzelany, N. Matłok, K. Lech, A. Figiel, *J. Food Sci. Technol.* **56** (2019) 2386–2394 (https://doi.org/10.1007/s13197-019-03656-2)
39. M. Pasławska, K. Sala, A. Nawirska-Olszańska, B. Stępień, E. Pląskowska, *Nat. Prod. Commun.* **15** (2020) (https://doi.org/10.1177/1934578X20904521).

Accepted manuscript